Pharmacological Research - Modern Chinese Medicine 10 (2024) 100399

Contents lists available at ScienceDirect

Pharmacological Research - Modern Chinese Medicine

journal homepage: www.elsevier.com/locate/prmcm

In-silico and *in-vivo* comparative evaluation of the cardioprotective potential of Yellow turmeric and White turmeric in Mn-induced cardiac oxidative stress

Toluwalope T. Fasooto [a,*], Oluwakemi R. Ogundana [a], Abiola F. Adebayo [a], David B. Olawade [b], Ezekiel A. Olugbogi [c,e], Oluwaseun Fapohunda [d,e], Afolabi C. Akinmoladun [a]

[a] *Biochemical and Molecular Pharmacology and Toxicology Laboratories, Department of Biochemistry, School of Life Sciences, The Federal University of Technology, P. M.B. 704, Akure 340110, Nigeria*
[b] *Department of Allied and Public Health, School of Health, Sport and Bioscience, University of East London, London, United Kingdom*
[c] *Molecular Laboratory and Simulation Center (Mols & Sims), Ado-Ekiti, Nigeria*
[d] *Chemistry and Biochemistry Department, University of Arizona, USA*
[e] *Department of Biochemistry, Adekunle Ajasin University, Akungba Akoko 001, Ondo State, Nigeria*

ARTICLE INFO

Keywords:
Manganese neurotoxicity
Oxidative stress
Yellow and white turmeric
Molecular docking

ABSTRACT

Introduction: The effect of the ethanol extracts of *Curcuma longa* Linn (yellow turmeric) and *Curcuma zedoaria* Rosc (white turmeric) on cardiac oxidative stress in rats exposed to manganese was evaluated in this study.
Methods: We divided 60 Wistar rats into 12 groups ($n = 5$) with some administered different concentrations of yellow or white turmeric extract. The animals except the control groups were exposed to manganese on days 1,3, and 7. All the animals were sacrificed on the 8th day and the hearts were harvested for biochemical assays. Ferric-reducing antioxidant power (FRAP) and the levels of cardiac superoxide dismutase, reduced glutathione, nitric oxide, and lipid peroxidation in rats were determined. Additionally, *in silico* studies were performed to further compare the cardioprotective potential of the two species of turmeric.
Results: The results showed that rats treated with manganese alone had decreased levels of FRAP, superoxide dismutase, and glutathione but increased levels of nitric oxide and lipid peroxidation were observed. The Mn-induced oxidative stress was ameliorated in animals co-treated with yellow or white turmeric. The yellow turmeric showed better activity than white turmeric. In the *in-silico* evaluation, phytocompounds from yellow turmeric had higher binding energy against Nuclear factor erythroid 2-related factor 2 (NRF2) protein than the ones from white turmeric. Bioactive compounds from white turmeric did not violate any of Lipinski's rules of five or three, despite having lower binding energy.
Conclusion: These findings suggest that ethanol extract of yellow and white turmeric may have the potential to ameliorate manganese-induced cardiac oxidative stress.

1. Introduction

Manganese (Mn) is an essential element required for the growth, development, and general maintenance of health. In the heart, Mn is an important cofactor for superoxide dismutase; an enzyme responsible for the transformation of superoxide into hydrogen peroxide (H_2O_2) which takes place in the matrix compartment of the heart mitochondria [1]. Humans generally are readily exposed to Mn from the soil, air, and waterways due to erosion, and from artificial and industrial sources. Furthermore, human exposure to Mn arises primarily from daily dietary

List of Abbreviations: Mn, Manganese; ROS, Reactive Oxygen Species; DMSO, Dimethyl Sulphoxide; GSH, Glutathione; CAT, Catalase; GPx, Glutathione peroxidase; RO5, Rule of five; TBARS, Thiobarbituric acid reactive substances; FRAP, Ferric reducing antioxidant power; NO, nitric oxide; LPO, lipid peroxidation; MMGBSA, Molecular mechanics with generalized Born and Surface area solvation.; HTVS, High throughput virtual screening; SSA, sulfosalicylic acid; CL, Curcuma longa; CZ, Curcuma zedoaria; ADMET, Absorption, Distribution, Metabolism, Excretion, and Toxicity; NRF2, Nuclear Factor Erythroid 2-Related Factor 2; SOD, Superoxide dismutase; VSMC, Vascular Smooth Muscle Cells.

* Corresponding author.
E-mail address: temitayotoluwalope@gmail.com (T.T. Fasooto).

https://doi.org/10.1016/j.prmcm.2024.100399
Received 16 November 2023; Received in revised form 17 February 2024; Accepted 20 February 2024
Available online 21 February 2024

intakes such as legumes, rice, and nuts [2]. Regardless of its essentiality, high-dose Mn accumulation can result in Manganism or Manganese toxicity (a toxic condition resulting from chronic exposure to manganese) and is reported to cause depression of cardiac myocytes and an increase in coronary vascular resistance [3]. Patients with manganism exhibit a variety of symptoms, including a decrease in blood pressure and heart rate [4].

Mn-induced cardiovascular dysfunction develops because of its accumulation in the mitochondrial matrix. Mn may disrupt mitochondrial function by inhibiting energy transduction, inducing mitochondrial DNA mutation, and enhancing the production of free radicals [5]. Mn accumulation in the mitochondria inhibits the electron transport chain complexes altering oxidative phosphorylation and ATP production [6]. The impaired energy production affects mitochondrial penetrability transition, causing the swelling of organelle, and the disruption of the outer membrane, leading to the release of various apoptogenic factors into the cytosol, thereby promoting apoptosis [6]. Degradation of high-energy phosphate is also accompanied by extreme generation of reactive oxygen species (ROS), which induces membrane polyunsaturated fatty acids oxidation, producing a line-up of lipid peroxidation products. Additionally, the production of ROS is accompanied by inflammatory responses and the release of inflammatory mediators which is associated with cardiovascular diseases [6]. The clinical manifestations of Mn intoxication are characterized by extrapyramidal dysfunction and neuropsychiatric symptoms [7]. Whereas Mn neurotoxicity is well recognized and documented, the effect of Mn on the cardiovascular system has received less attention. Oxidative stress, characterized by the generation of reactive oxygen species (ROS) is a linking point of several other mechanisms of manganese toxicity [8].

Turmeric commonly referred to as “Jianghuang” in China has long been used in traditional Chinese medicine (TCM) [9]. It is used in the preparation of different Chinese herbal products. For instance, it is the main component of Xierriga-4 decoction which is a well-known herbal medicine for the treatment of urinary diseases and pain [10]. *Curcuma longa* and *Curcuma zedoaria* are known as yellow turmeric and white turmeric, respectively, and both widely utilized in TCM. They hold significant therapeutic values owing to their diverse pharmacological properties. These Curcuma species have been traditionally employed in TCM and reported to possess anti-inflammatory and cardioprotective effects [11,12]. Extract from turmeric has been revealed to possess antioxidant, anti-inflammatory, and cardioprotective properties [13]. However, there is limited data available on the cardio-protective potentials of turmeric in manganese-induced cardiotoxicity. Therefore, this study aimed to evaluate the effect of *Curcuma longa* Linn and *Curcuma zedoaria* Rosc ethanol extracts (CL and CZ) on manganese-induced cardiac oxidative stress in rats. Furthermore, to assess the agonistic impact of CL and CZ’s compounds against the Nuclear Factor Erythroid 2-Related Factor 2 (Nrf2), this work used molecular docking, a crucial technique in structural molecular biology and computer-assisted drug development. In ascertaining the binding process and affinity of small molecules to a protein, molecular docking predicts the small molecule’s lowest energy conformation at the protein’s binding site [14]. Among the methods used are receptor grid construction, molecular docking, ADME-Tox Screening, MM/GBSA, target retrieval from a PDB database, and ligand library building and preparation from an online database. To find prospective therapeutic candidates and comprehend the cellular mechanisms behind protein-ligand interactions, a computational tool was utilized for the study.

2. Materials and methods

2.1. Chemicals

Thiobarbituric acid (TBA), trichloroacetic acid (TCA), adenosine triphosphate (ATP), 5,5′-dithiobis-(2-nitrobenzoic acid) (DTNB), ethylenediaminetetraacetic acid (EDTA), epinephrine, 2,3,5-triphenyl-1,3,4-triaza-2-azoniacyclopenta-1,4-diene chloride (TPTZ), reduced nicotinamide adenine dinucleotide (NADH), Griess reagent, and 4-aminosalicylic acid (PAS) were obtained from Sigma-Aldrich (St-Louis, MO, USA). Ethanol, formalin, hydrogen peroxide, and dimethyl sulphoxide (DMSO) were obtained from Scharlau (Scharlab S.L, Spain). All other chemicals and reagents used for this work were of analytical grade and were obtained from other standard commercial suppliers in Nigeria. The assay kit for total protein concentration determination was a product of Randox Laboratory Ltd (Antrim, UK).

2.2. Preparation of extracts

Fresh rhizomes of *Curcuma longa* and *Curcuma zedoaria* were obtained from Ibule and Owena, Ondo State, Nigeria, and duly authenticated at the Department of Crop Soil and Pest Management, the Federal University of Technology, Akure, Nigeria. The extraction of the active ingredients from the rhizomes of *Curcuma longa* and *Curcuma zedoaria* rhizomes was carried out using the Soxhlet apparatus. The rhizomes were washed, sliced, and spread on separate trays with a layer of thickness of approximately 0.15 cm. The rhizomes were air-dried in the shade at an ambient laboratory temperature of about 25 °C for 14 days [15]. Dried rhizomes were pulverized with an electric blender. Soxhlet extraction was performed as follows: 40 g of the turmeric powder was weighed and embedded in a thimble and put in the Soxhlet apparatus which was gradually filled with ethanol as the extraction solvent. Upon completion of the extraction, the ethanol was separated from the extract using a rotary evaporator.

2.3. Experimental animals

Male Wistar rats weighing 180 ± 20 g, used for the experiment, were housed in the Animal House of the Department of Biochemistry, Federal University of Technology, Akure, Nigeria. The rats were housed in plastic cages in a well-ventilated room and supplied with rat chow and water ad-lib. The animal management and experimental design followed the general guidelines of the National Institutes of Health for the Care and Use of Laboratory Animals in scientific investigations and were approved by the University’s Research Ethical Committee, Center for Research and Development (CERAD), Federal University of Technology, Akure, Nigeria.

2.4. Experimental design

The animals were divided into 12 groups with 5 animals per group and treated as follows:

Group I (Control). Saline

Group II. Mn (MN)

Group III. Mn + 200 mg/kg body weight (bw) *Curcuma longa* (MN + CL)

Group IV. Mn + 400 mg/kg bw*Curcuma longa* (MN +CL)

Group V. Mn + 200 mg/kg body weight (bw) *Curcuma zedoaria* (MN +CZ)

Group VI. Mn + 400 mg/kg bw*Curcuma zedoaria* (MN +CZ)

Group VII. Mn + 200 mg/kg bw PAS (MN + PAS)

Group VIII. 200 mg/kg bw*Curcuma longa* (CL 200)

Group IX. 400 mg/kg bw*Curcuma longa* (CL 400)

Group X. 200 mg/kg bw*Curcuma zedoaria* (CZ 200)

Group XI. 400 mg/kg bw*Curcuma zedoaria* (CZ 400)

Group XII. 200 mg/kg bw PAS (PAS)

The animals received three intraperitoneal doses of 100 mg/kg $MnCl_2$ (days 1, 3, and 7). Animals in the turmeric-administered groups received turmeric orally for 8 consecutive days. Thereafter, on day 9, the animals were sacrificed by cervical dislocation, and the heart was harvested and processed for biochemical estimations.

2.5. Relative heart weight

All rats were weighed immediately before being sacrificed and the hearts were weighed after excision. The two values were used to determine the relative heart weight.

2.6. Biochemical assays

Animals were sacrificed by cervical dislocation. Hearts were removed and washed in ice-cold 1.15 % (v/v) potassium chloride solution, blotted with filter paper, and weighed. They were then homogenized in 10% phosphate-buffered saline PBS (pH 7.4) (1:10 w/v) using a Teflon homogenizer. The resulting homogenate was centrifuged at 10,000 x g at 4 °C for 30 min to obtain the supernatant which was used for biochemical analyses.

2.6.1. Total protein concentration

Determined by the Biuret method (Weichselbaumin, 1995). We used an assay kit supplied by Randox Laboratories Ltd (Antrim, UK). The assay was conducted following the manufacturer's instructions.

2.6.2. Determination of reduced glutathione (GSH) level

The method of Beutler [16] was followed in estimating the level of reduced glutathione (GSH). Heart homogenate (50 µl) was added to 450 µl of distilled water and mixed with 750 µl of 4 % sulfosalicylic acid (SSA). The mixture was allowed to stand for 5 min and then filtered. We added 1 ml of filtrate to 4 ml of 0.1 M phosphate buffer (pH 7.4). Finally, 0.5 ml of Ellman's reagent was added. The absorbance was read at 412 nm against a reagent blank. GSH was proportional to the absorbance at that wavelength and the estimate was obtained from a GSH standard curve.

2.6.3. Determination of lipid peroxidation level

The extent of lipid peroxidation was evaluated by measuring the formation of thiobarbituric acid reactive substances (TBARS) according to the method of Varshney and Kale (1990). Heart homogenate (0.2 ml) was mixed with 0.8 ml of Tris-KCl buffer to which 0.25 ml of 30 % TCA was added. Then, 0.25 ml of 0.75 % TBA was added, and the mixture was placed in a water bath for 45 min at 80 °C. This was then cooled in ice and centrifuged at 3000 g for 10 min. The clear supernatant was collected, and absorbance was measured against a reference blank of distilled water at 532 nm. Lipid peroxidation in units/mg protein was computed with a molar extinction coefficient of 1.56×10^5.

2.6.4. Ferric reducing antioxidant power

The ferric-reducing antioxidant power was determined as described by Patil [17]. 250 µL plasma sample was mixed with 250 µL 200 mM sodium phosphate buffer (pH 6.6) and 250 µL 1 % potassium ferricyanide. The mixture was incubated at 50 °C for 20 min. and then 250 µL 10 % trichloroacetic acid was added. This mixture was centrifuged at 650 rpm for 10 min. We mixed 50 µL of the supernatant with an equal volume of water and 1 mL 0.1 % ferric chloride. The absorbance was measured at 700 nm in the spectrophotometer. Then, the ferric-reducing antioxidant property was subsequently calculated as an ascorbic acid equivalent.

2.6.5. Determination of nitric oxide level

Nitrite and nitrate estimations in biological material are commonly used as a marker for nitric oxide (NO) production. The nitrite level was estimated in heart homogenates using the Griess reaction [18]. Briefly, the homogenate was centrifuged at 1580 g for 15 min at 4 °C and the supernatant thus obtained was deproteinized by mixing with an equal amount of 4% sulfosalicylic acid. Further, 350 µl of this reaction mixture was mixed with 350 µl of Griess reagent and incubated for 10 min. The absorbance of the samples was measured at 540 nm using a spectrophotometer. Nitrite concentrations were calculated using a calibration curve prepared from sodium nitrite and expressed as pmol/mg of protein in tissue homogenate.

2.6.6. Determination of superoxide dismutase (SOD) enzyme activity

The activity of SOD in the homogenates was determined by the method of Kakkar [19]. The tissue homogenate (1 mL) of the various groups was diluted in 9 ml of distilled water to make 1 in 10 dilutions. An aliquot of the diluted sample was added to 2.5 ml of 0.05 M carbonate buffer (pH 10.2) to equilibrate in the spectrophotometer and the reaction was initiated by the addition of 0.3 ml of freshly prepared 0.3 mM adrenaline was quickly mixed by inversion. The reference cuvette contained 2.5 ml of buffer, 0.3 ml of the substrate (adrenaline), and 0.2 ml of water. The increase in absorbance at 480 nm was monitored every 30 s for 150 s.

2.7. In-silico analysis

2.7.1. Molecular docking

All computational experiments, such as High throughput virtual screening (HTVS), molecular docking, MMGBSA, and visualization, were done with Maestro Schrodinger version 12.8 software.

2.7.2. Protein preparation

The three-dimensional crystal structure of Nrf2 was modeled using PDB ID: 5CGJ [20]. The target protein (Nrf2) was given bond instructions and had hydrogen atoms added. Using the Protein Preparation Wizard of Schrödinger Suite 2021, water molecules within 5 of the ligands were removed from the protein-ligand complex's structure [21]. In addition, side chains and loops missing from the prime tool were repaired. By producing tautomeric states at a neutral pH and employing the OPLS4 force field to limit minimization, Nrf2 was further enhanced. It was decided to use the ready Nrf2 for molecular docking.

2.7.3. Receptor grid generation

The binding direction and size of the active site are determined by receptor grid generation for protein-ligand docking. The scoring coordinates of the Nrf2 binding pocket were determined using Schrödinger Maestro 12.8′s receptor grid generation module [21] based on the co-crystallized ligand. The x, y, and z grids' coordinates are 40.07, −20.39, and −4.89, respectively.

2.7.4. Ligand preparation

Their bioactive compounds from Curcuma longa and Curcuma zedoaria (yellow and white turmeric) were acquired from published literature, and the 2D structures of the bioactive compounds from Curcuma longa and Curcuma zedoaria and the reference compound were retrieved from the NCBI PubChem database (https://pubchem.ncbi.nlm.nih.gov). The ligands were prepared using the LigPrep function of the Schrodinger suite in the OPLS4 forcefield. When the Epik module was used to create the compounds' ionization states, just one stereoisomer per ligand was created at a pH of 7.0 ± 2.0. The Nrf2 Co-ligand (3s)-1-(4-[(2,3,5,6-Tetramethylphenyl) sulfonyl] amino naphthalen-1-Yl] pyrrolidine-3-Carboxylic Acid) was also discovered and downloaded from PubChem. It was then synthesized identically to the other ligands

and used as a reference drug.

2.8. Statistical analysis

Results were analyzed using appropriate analysis of variance (ANOVA) followed by Duncan's multiple range test applied where appropriate. In all the tests, $P < 0.05$ was taken as the criterion for statistical significance. The statistical software used to analyze the data was GraphPad Prism 6.01 (GraphPad Software Inc, CA, USA).

2.9. Ethical approval

The study was conducted following the ethical guidelines set forth by the University's Research Ethical Committee, Center for Research and Development (CERAD), Federal University of Technology, Akure, Nigeria. The study was assigned the animal protocol number FUTA/ETH/20/28.

3. Results

3.1. Effects of turmeric rhizome extract on reduced glutathione (GSH) level in the heart of manganese-toxified rats

The effects of the extracts of *Curcuma longa* Linn and *Curcuma zedoaria* Rosc on reduced glutathione (GSH) levels in the hearts of rats exposed to manganese toxicity are shown in Fig. 1. The GSH concentration decreased significantly in the heart of the Mn-toxified group compared to the control group. Induced animals treated with selected plant extracts increase the concentration of GSH in the heart. This increase was significant in the MN + CZ 400 group. CL significantly increased GSH levels in normal rats.

3.2. Extracts of turmeric rhizomes ameliorate Mn-induced lipid peroxidation in the heart of rats

The effect of the extract of *Curcuma longa* (CL) and *Curcuma zedoaria* (CZ) on lipid peroxidation (LPO) in the hearts of rats exposed to manganese is shown in Fig. 2. The MDA level increased significantly in the Mn-toxified group compared to the control group. Treatment of animals with turmeric extracts significantly decreased the level of MDA produced in the heart. This reduction is most significant in the MN + CL 200 group. The result also showed that different doses of CL and CZ did not adversely affect MDA levels in normal animals used in this study.

3.3. Effects of turmeric rhizome extract on the cardiac ferric-reducing antioxidant power of manganese-toxified rats

The effects of the extracts of *Curcuma longa* Linn and *Curcuma zedoaria* Rosc on the ferric-reducing antioxidant power in the hearts of rats exposed to manganese toxicity are shown in Fig. 3. The ferric-reducing antioxidant power decreased significantly in the heart of Mn-administered rats compared to the control group. Treatment of animals with the extracts significantly increased the ferric-reducing antioxidant power in the heart. Again, the increase was most significant in the MN + CL 200 group.

3.4. Effects of turmeric rhizome extract on the nitric oxide level in the heart of manganese-toxified rats

The effect of the extract of *Curcuma longa* Linn and *Curcuma zedoaria* Rosc on the nitric oxide (NO) level in the hearts of rats exposed to manganese toxicity is shown in Fig. 4. The NO level increased significantly in the heart of Mn-toxified rats compared to the control group. Treatment of induced animals with plant extracts significantly decreases the level of NO in the heart. The reduction was most significant in the MN + CZ 200 and MN + CL 200 groups.

3.5. Effects of turmeric extracts on cardiac superoxide dismutase (SOD) activity of manganese-administered rats

The effects of the extracts of *Curcuma longa* and *Curcuma zedoaria* on the activity of superoxide dismutase in the hearts of rats exposed to manganese toxicity are shown in Fig. 5. The cardiac SOD activity decreased significantly in the heart of Mn-toxified rats compared to the control group. Treatment with turmeric extracts significantly increased the activity of SOD in the heart. This increase is most significant in the MN + CL 200 group.

4. Discussion

4.1. In vivo studies

Botanicals have been the source of hope for rural dwellers since time immemorial. The use of turmeric in traditional Chinese medicine has been reported in the literature [22]. Jianghuang is one of the primary ingredients utilized in the composition of some renowned Chinese patent medications, such as Wuzi Yanzong Wan (herbal formula), Shujin Huoxue, Shugan Jianpi (pills). Folkloric use of turmeric has been

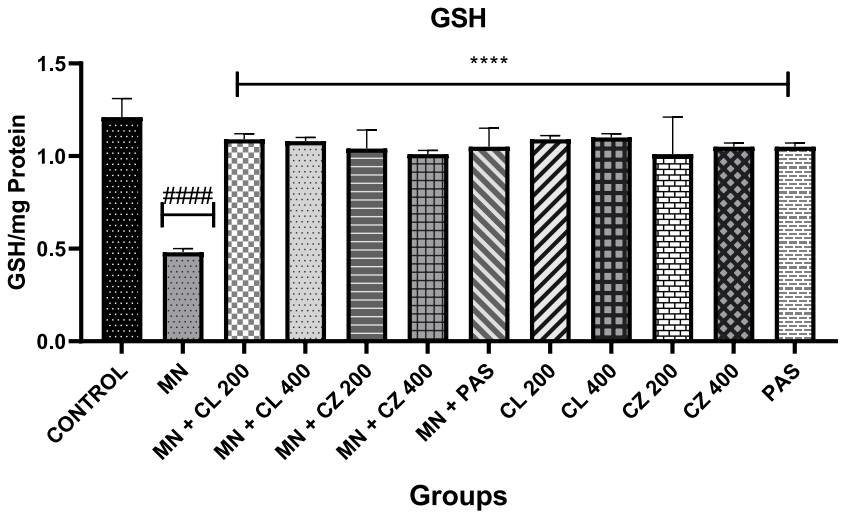

Fig. 1. Effects of turmeric rhizome extract on reduced glutathione (GSH) level in the heart of manganese-administered rats (results are expressed as mean ± SD ($n = 5$). $^{\#\#\#\#}p < 0.0001$ vs control; $^{****}p < 0.0001$ vs Manganese, CL: *Curcuma longa*, CZ: *Curcuma zedoaria*, PAS: p-aminosalicylic acid).

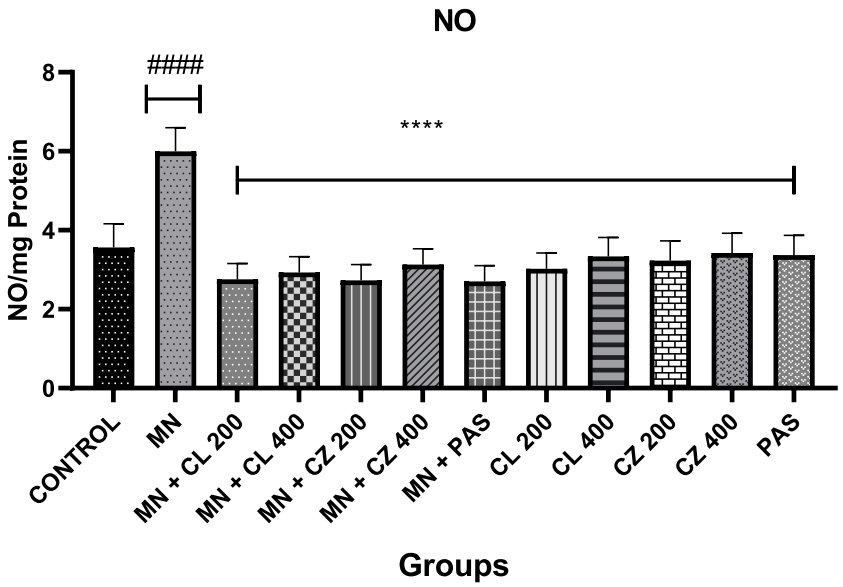

Fig. 2. Effects of turmeric rhizome extract on lipid peroxidation level in the heart of manganese-administered rats (results are expressed as mean ± SD ($n = 5$). $^{\#\#\#\#}p < 0.0001$ vs control; $^{****}p < 0.0001$ vs Manganese, CL: *Curcuma longa*, CZ: *Curcuma zedoaria*, PAS: p-aminosalicylic acid).

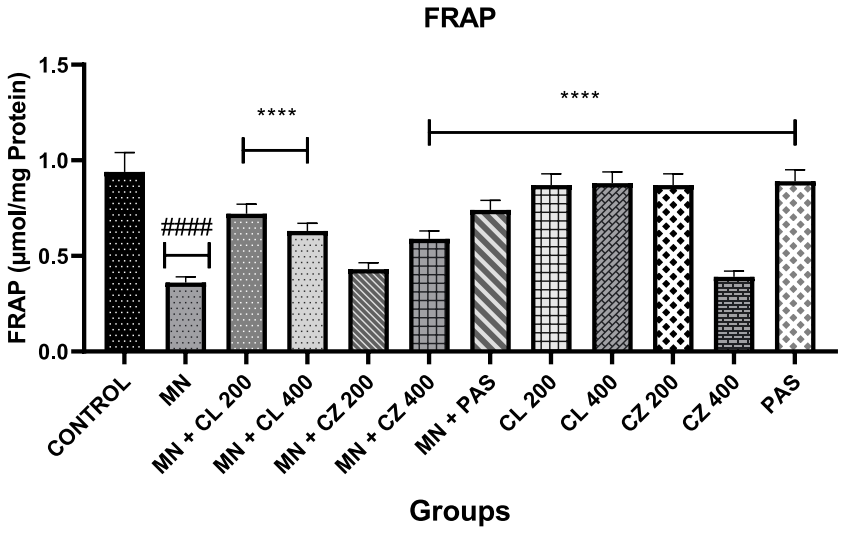

Fig. 3. Effects of turmeric rhizome extract on the Ferric reducing antioxidant power in the heart of manganese-administered rats (results are expressed as mean ± SD ($n = 5$). $^{\#\#\#\#}p < 0.0001$ vs control; $^{****}p < 0.0001$ vs Manganese, CL: *Curcuma longa*, CZ: *Curcuma zedoaria*, PAS: p-aminosalicylic acid).

reported in the literature. Different species of turmeric have also been investigated for various health benefits. Some of these benefits range from neuroprotective and nephroprotective to hepatoprotective effects [23,24,25,26]. Zeng and co [27] also published on the efficacy and safety of curcumin and CL extract in the treatment of arthritis by reducing severe inflammation and pain levels. However, the cardioprotective effect of CL and CZ is yet to be extensively investigated in Mn-toxified rats. This study investigated the cardioprotective potential of two species of turmeric. Five different biochemical parameters were assessed. These include LPO, SOD, GSH, FRAP, and NO levels. Lipid peroxidation was proposed as one of the molecular mechanisms by which heavy metals induce toxicity [28]. Malondialdehyde (MDA) is one of the hallmarks of lipid peroxidation. An increase in the level of free radicals in a system leads to increased lipid peroxidation which is usually indicated by the increased MDA level in the system. MDA is a well-known marker of oxidative stress [29].

Various studies have reported that Mn toxicity increases MDA levels [30]. Specifically, Mn toxicity was recently confirmed by increased MDA levels in the chicken liver [30]. We observed the same trend in this present study as in Fig. 1. The MDA level increased significantly in the MN group. This may be partly due to its action on aconitase, which participates in cellular iron regulation and mitochondrial energy production [31]. MDA was significantly reduced with the treatment of CL and CZ. The MN + 200 CL group showed the most significant restoration of the MDA level to normal. This is possible because of the flavonoid content of the turmeric plants. An earlier study reported that different varieties of turmeric plants are rich in flavonoids [32]. Another study further corroborated that turmeric flavonoids are mainly curcumin and its derivatives [33]. Alizadeh and Kheirouri reported in their studies that curcumin was able to reduce MDA levels [30]. Curcumin is an important flavonoid that may be used as an adjunct therapy in individuals with oxidative stress.

SOD is an antioxidant enzyme that is commonly assessed to check the level of antioxidant activity in a tissue or organ (Chen et al., 2017). Several studies investigated the activities of SOD to check the effect of their treatment on different subjects [34]. We investigated the levels of

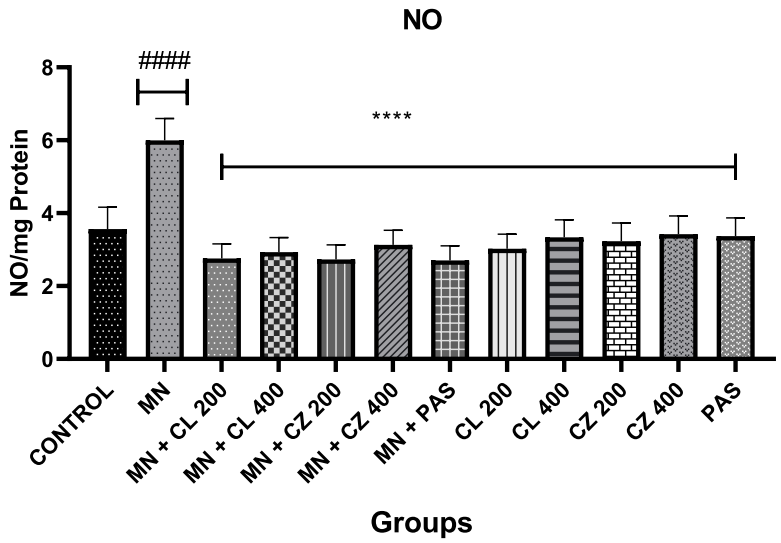

Fig. 4. Effects of turmeric rhizome extract on the Nitric oxide level in the heart of manganese-toxified rats (results are expressed as mean ± SD ($n = 5$). $^{\#\#\#\#}p <$ 0.0001 vs control; $^{****}p < 0.0001$ vs Manganese, CL: *Curcuma longa*, CZ: *Curcuma zedoaria*, PAS: p-aminosalicylic acid).

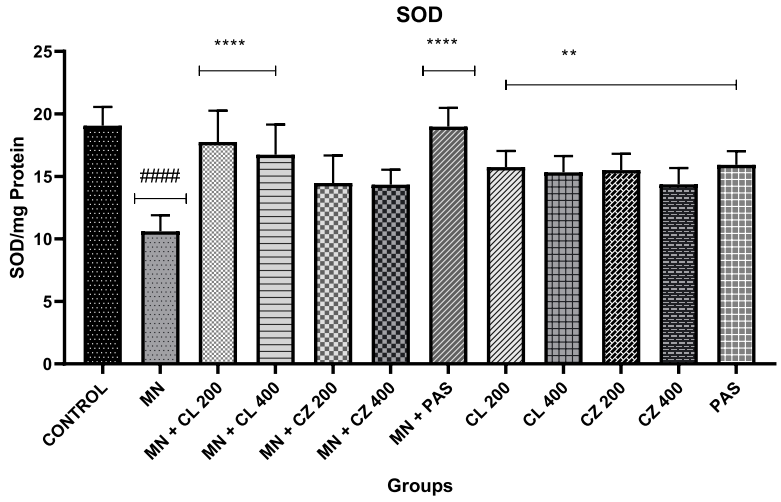

Fig. 5. Effects of turmeric rhizome extract on cardiac Superoxide dismutase (SOD) activity of manganese-toxified (results are expressed as mean ± SD ($n = 5$). $^{\#\#\#\#}p$ < 0.0001 vs control; $^{****}p < 0.0001$ vs Manganese, CL: *Curcuma longa*, CZ: *Curcuma zedoaria*, PAS: p-aminosalicylic acid).

SOD activity in the heart of rats, and we found that SOD was significantly reduced in the MN group (see Fig. 5). This is due to the oxidative stress induced by manganese in the research animals. Turmeric extracts were able to restore the SOD activity in the Mn-toxified rats. This is possible because of their curcumin content's ability to upregulate Nuclear Factor E2-related factor-2 (Nrf2). Levonen and colleagues found a similar result when they worked on the transduction of vascular smooth muscle cells (VSMCs) with Nrf2-expressing adenovirus increased the expression of several antioxidant enzymes [35]. Generally, curcumin activates Nrf2 by its the Michael reaction of its electrophilic moieties with the thiol residues of Keap1. Nrf2 in turn induces the transcription of SOD and other antioxidant enzymes [36].

Another important antioxidant enzyme is reduced GSH. It is commonly reported that GSH activity is reduced in Mn-toxified subjects [36]. We found the same trend in our study. This is because of the presence of oxidative stress and inadequate antioxidant defense mechanisms in rats induced with Mn [36]. The trend was reversed in the CZ and CL-treated groups, suggesting that the plant contains important phytochemicals that may serve as a powerful antioxidant by upregulating Nrf2 activity [35]. FRAP assay is used to investigate the oxidant-reducing potential of a sample. It is based on the ability of the antioxidants in a sample to donate electrons to the ferric complex leading to the conversion of $Fe^{3+}$to Fe^{2+}-TPTZ complex thereby terminating the radical chain reaction (7). The higher FRAP value of the MN + CL 200 group indicates that yellow turmeric has robust antioxidant potential. This result agrees with the reports described by Tekin and colleagues [37].

Another biochemical parameter that is usually checked in the case of toxicity is the NO level in the system. Increased NO levels are indicative of oxidative stress in a system. In our study, we discovered that the NO level was significantly increased by the administration of Mn. This agrees with a recent study [26]. However, this condition was significantly reversed by turmeric extracts. This may be due to the curcumin content of these plant extracts. It is well established that curcumin has scavenging potential on NO [30]. Overall, looking at the biochemical parameters investigated in this present study, turmeric extracts offer a better ameliorative potential for the treatment of Mn-induced cardiotoxicities than PAS [13].

4.2. *In-silico studies*

In silico, in vitro, and *in vivo* studies all play important roles in

understanding the biological effects of molecules [38,39]. The *in silico* study predicted favorable binding affinity of the compounds with target protein residues with high docking scores against Nuclear factor erythroid 2-related factor 2 (NRF2) protein (Figs. 6–9) while comparing white and yellow turmeric. Numerous studies have demonstrated that *in silico* studies can complement and enhance traditional *in vivo* studies [40]. *In silico* methods provide a valuable platform for predicting and understanding biological phenomena, guiding experimental design, and reducing the time and cost associated with experimental research. Furthermore, the integration of *in silico* and *in vivo* approaches allows researchers to leverage the strengths of both methods, leading to a more comprehensive understanding of biological processes and accelerating the drug discovery and development pipeline.

In this work, the systemic comparative evaluation of the cardioprotective potential of yellow and white turmeric in Mn-induced cardiac oxidative stress was determined.

NRF2 is a transcription factor that controls the expression of antioxidant enzymes in response to oxidative stress. Computational tools were also used to assess the plant's species [41]. Superoxide dismutase, catalase, and glutathione peroxidase are a few antioxidant enzymes that are activated by NRF2 and function to defend cells from oxidative damage by neutralizing free radicals [42,43]. Phase II enzymes and other enzymes involved in the detoxification of hazardous chemicals are regulated in expression by NRF2. According to studies, activating NRF2 can boost the production of antioxidant enzymes and shield cells from oxidative damage. NRF2 activators are being investigated by some researchers as a potential treatment approach for disorders including cancer and neurological diseases that are aggravated by oxidative stress [44]. To completely comprehend the function of NRF2 in these illnesses and to establish the efficacy and safety of NRF2 activators as a therapy option, additional study is nonetheless required. Lee and colleagues [35] also affirmed that the transcription factor called NRF2 (nuclear factor erythroid 2-related factor 2) controls the expression of antioxidant enzymes in response to oxidative stress [35].

Several antioxidant enzymes, including glutathione peroxidase, catalase, and superoxide dismutase (SOD), are activated by NRF2 via transcription. SOD is an enzyme that speeds up the process of turning superoxide into oxygen and hydrogen peroxide [36]. Superoxide is a very reactive form of oxygen that can harm tissues and cells. SOD aids in the protection of cells against oxidative stress by neutralizing superoxide. An enzyme called CAT helps hydrogen peroxide break down into water and oxygen [37]. By neutralizing hydrogen peroxide, CAT, like SOD, assists in preventing oxidative stress on cells. GPx is an enzyme that uses reduced glutathione to catalyze the reduction of organic hydroperoxides and hydrogen peroxide. GPx neutralizes reactive oxygen species such as hydrogen peroxide to protect cells from oxidative stress [45]. An enzyme called GRx is involved in the body's detoxification of toxic chemicals [46]. Glutathione disulfide (GSSG) is converted to reduced glutathione by GRx because of its involvement (GSH). According to studies, NRF2 activation can boost the production of SOD, CAT, GPx, and GRx as well as shield cells from oxidative stress. NRF2 activators are being investigated by some researchers as a potential treatment approach for disorders including cancer and neurological diseases that are aggravated by oxidative stress [47]. To completely comprehend the role of NRF2 in these illnesses and to assess the efficacy and safety of NRF2 activators as a therapy option, additional study is necessary [48].

4.3. Molecular docking and MM/GBSA

Molecular docking is a computational technique used in drug discovery and design to predict the preferred orientation and binding affinity of a small molecule (ligand) within a target macromolecule (usually a protein) [49]. The goal is to understand and optimize the interactions between the drug candidate and its target, providing insights into the potential efficacy of the compound. The binding of ligands from CL and CZ to the active site of NRF2, following molecular docking simulations, instigates a cascade of molecular and cellular events, influencing the transcriptional activity of NRF2 and ultimately impacting cellular fate. To further connect our understanding, Molecular Mechanics/Generalized Born Surface Area (MM/GBSA) analysis comes into play [50], offering a deeper exploration of the thermodynamics underlying these ligands binding and its implications on NRF2 activation. The thermodynamic parameters obtained from MM/GBSA directly correlate with cellular consequences. Favorable binding energies align with increased transcriptional activation of NRF2 target genes [51]. The upregulation of antioxidant enzymes and detoxification pathways, crucial facets of NRF2-mediated responses, can be rationalized by the thermodynamic stability conferred by ligand binding.

The MM-GBSA module, which is integrated with the Schrodinger suite's prime program, was used to compute the ΔGbind for Nrf2-lead ligand complexes. Following the docking analysis, the ΔGbind was used to calculate the free binding energy for the screened compounds using advanced mechanics [52]. MM-GBSA technique is a reliable post-docking method for estimating the binding position of docked complexes, according to several researchers [53]. Stachyurin, 1-o-Caffeoylglucose, trans-o-Coumaric acid 2-glucoside, l-Arabinose, Isorhamnetin, and the reference ligand had −11.87, −9.962, −9.356, −7.287, −6.965, and −6.642 (Kcal/mol) docking scores and −82.64, −48.33, −57.59, −30.94, −33.35 and −76.92 (ΔGbind) MM-GBSA scores respectively for yellow turmeric (Fig. 6), and Curcuminoid, (-)-Isoborneol, Borneol, Curcuminoid, Spathulenol for white turmeric had docking scores ranging from −6.179 to −3.809 and −49.16 to −37.18 according to the MM-GBSA output (Fig. 8) [54].

According to these results, yellow turmeric has some of the best bioactive compounds with high binding affinities with the pocket of Nrf2 agonists; stachyurin had the best MM/GBSA and docking score of all the screened compounds, suggesting that it may have drug-like properties for detoxifying manganese toxicity. Although the active ingredient in yellow turmeric, stachiyurin, violated three of Lipinski's

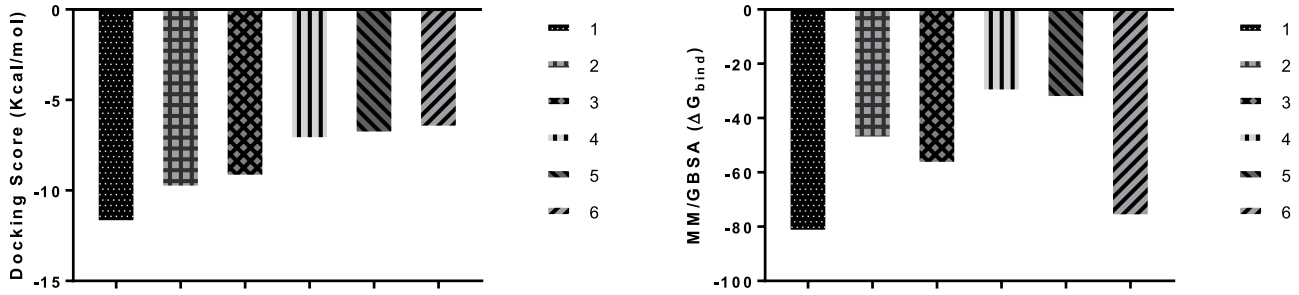

Fig. 6. Docking score (kcal/mol) and MM/GBSA score ($\Delta G_{bind,}$ kcal/mol) of the top five ligands obtained from yellow turmeric against Nrf2 compared to the co-crystalized ligand ((3s)-1-(4-{[(2,3,5,6-Tetramethylphenyl) sulfonyl] amino} naphthalene-1-Yl) pyrrolidine-3-Carboxylic Acid) in black color (6). Stachyurin in blue (1), 1-o-Caffeoylglucose in green (2), trans-o-Coumaric acid 2-glucoside in yellow (3), l-Arabinose in ash-grey (4), and Isorhamnetin in orange (5) which implies the binding energy.

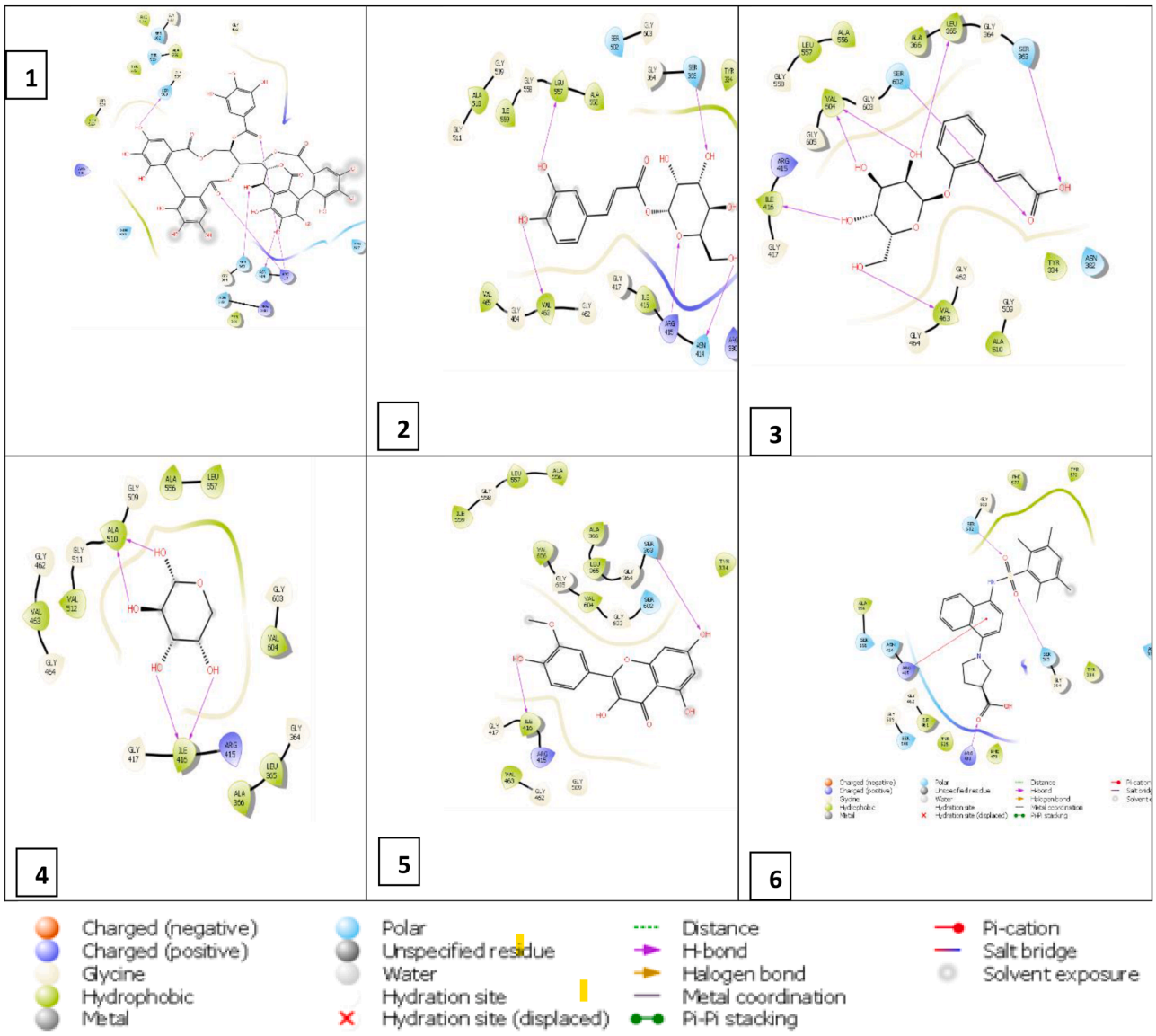

Fig. 7. Molecular interaction between the active site of the protein target (Nrf2) and the ligands obtained from yellow turmeric 1-6. Stachyurin (1), 1-o-Caffeoyl-glucose (2), trans-o-Coumaric acid 2-glucoside (3), L-Arabinose (4), Isorhamnetin (5), and the co-crystalized ligand (3s)-1-(4-{[(2,3,5,6-Tetramethylphenyl) sulfonyl] amino} naphthalene-1-Yl) pyrrolidine-3-Carboxylic Acid (6) respectively.

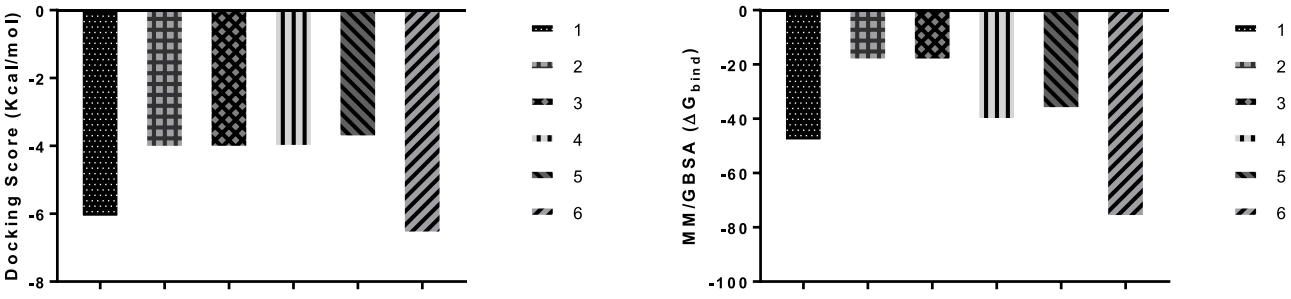

Fig. 8. Docking score (kcal/mol) and MM/GBSA score (ΔG_{bind}, kcal/mol) of the protein target (Nrf2) and the ligands obtained from white turmeric 1-6. Curcuminoid 004 (1), (-)-Isoborneol (2), Borneol (3), Curcuminoid 005 (4), Spathulenol (5), and the co-crystalized ligand (3s)-1-(4-{[(2,3,5,6-Tetramethylphenyl) sulfonyl] amino} naphthalene-1-Yl) pyrrolidine-3-Carboxylic Acid (6) respectively.

five rules, making it poisonous and perhaps unsuitable as a drug-like substance. With a high binding affinity (−11.87 kcal/mol) for the Nrf2 active site and an MM/GBSA score of −82.64 kcal/mol, stachyurin, if structurally modified (molecular weight of 936.657), has a high likelihood of becoming a standard drug. This study also suggests that further research and structural modification on stachyurin could make it a suitable compound and serve as an Nrf2 agonist. While the reference ligand ((3s)-1-(4-[(2,3,5,6-Tetramethylphenyl) sulfonyl] amino

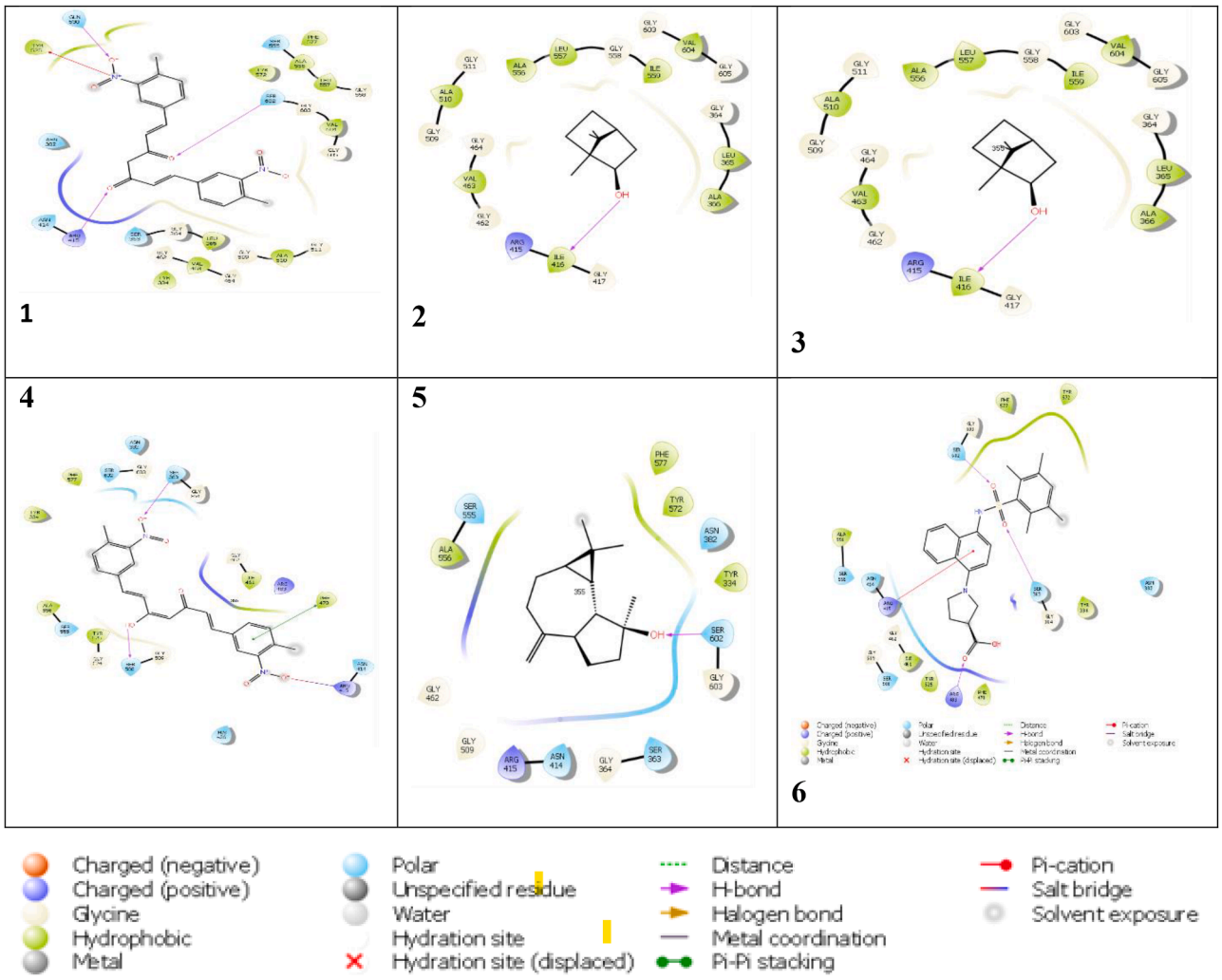

Fig. 9. Molecular interaction between the active site of the protein target (Nrf2) and the ligands obtained from white Tumeric 1-6. Curcuminoid (1), (-)-Isoborneol (2), Borneol (3), Curcuminoid (4), Spathulenol (5), and the co-crystalized ligand (3s)-1-(4-{[(2,3,5,6-Tetramethylphenyl) sulfonyl] amino} naphthalene-1-Yl) pyrrolidine-3-Carboxylic Acid (6) respectively.

naphthalene-1-Yl) pyrrolidine-3-Carboxylic Acid) performed well with a docking score of −6.642, white turmeric had curcuminoid as its lid molecule. Despite having a lower MM/GBSA score than the co-crystallized one, the compound passed the ADMET test and complied with all of Lipinski's rules of five and three (Table 1).

4.4. Molecular interaction

The interaction between two molecules during the docking process typically a ligand and a receptor is referred to as the molecular interaction in a docking procedure. These interactions are crucial for drug research and design because they aid in predicting the affinity and

Table 1
This shows the result of the ADMET test conducted using Qikprop which includes but is not limited to Rule of five (Ro5), Rule of three (Ro3), PSA, and molecular weight for both the white and yellow turmeric simultaneously. Entry 1 represents the white turmeric while (CZ) Entry 2 represents the yellow turmeric (CL).

Entry 1	mol MW	PISA	donorHB	QPlogHERG	QPPCaco	QPlogBB	QPPMDCK	QPlogKp	QPlogKhsa	PSA	Ro5	Ro3
Curcuminoid 004	394.383	227.361	0	−6.129	36.432	−2.831	13.787	−4.49	0.249	138.267	0	0
(-)-Isoborneol	154.252	0	1	−2.207	4466.361	0.238	2493.866	−2.096	−0.106	19.195	0	0
Borneol	154.252	0	1	−2.207	4466.361	0.238	2493.866	−2.096	−0.106	19.195	0	0
Curcuminoid 005	394.383	238.253	0	−6.155	32.75	−2.933	12.288	−4.445	0.754	131.38	0	1
Spathulenol	220.354	30.943	1	−2.925	4925.407	0.253	2772.03	−1.904	0.657	20.521	0	0

Entry 2	mol MW	PISA	donorHB	QPlogHERG	QPPCaco	QPlogBB	QPPMDCK	QPlogKp	QPlogKhsa	PSA	Ro5	Ro3
Stachyurin	936.657	165.423	16	−5.466	0.001	−8.187	0	−12.964	−1.259	475.813	3	2
1-o-Caffeoylglucose	342.302	140.296	6	−5.064	16.19	−2.991	5.738	−5.385	−1.061	166.557	1	1
trans-o-Coumaric acid 2-glucoside	326.302	158.527	5	−2.708	7.718	−2.414	3.277	−4.883	−1.11	147.301	0	1
L-Arabinose	150.131	0	4	−2.087	202.53	−0.951	88.054	−4.419	−0.766	95.271	0	0
Isorhamnetin	316.267	231.278	3	−5.118	87.927	−1.751	35.733	−4.212	−0.178	123.39	0	0

specificity of the ligand-receptor interaction [55]. Hydrogen bonds, van der Waals contacts, and electrostatic interactions are just a few of the several kinds of molecular interactions that can take place during docking. Because they influence the binding affinity and specificity of the ligand-receptor interaction, these interactions are crucial. When the electrons of a hydrogen atom are shared with another atom, a sort of interaction known as hydrogen bonding takes place.

This interaction is significant because it frequently serves as a predictor of the affinity and specificity of ligand-receptor interaction and because it can create a solid link between two molecules. Due to the alterations in their electron clouds, two molecules experience attractive Van der Waals interactions. These interactions are crucial because they can create a weaker but still powerful binding between two molecules and because they can be utilized to forecast the affinity and specificity of ligand-receptor interaction. When positive or negative charges are present, electrostatic interactions between molecules result in forces. These interactions are significant because they can influence the specificity and binding affinity of ligand-receptor interaction and because they can be utilized to anticipate these properties. In general, the molecular interactions in the docking process are significant because they aid in the prediction of the affinity and specificity of ligand-receptor interaction, both of which are essential in the design and development of drugs [56].

The ligand-Nrf2 complexes result in inter and intramolecular interactions such as hydrogen bonding, pi-pi stacking, pi-cation, and salt bridges [57]. The best five bioactive molecules of yellow and white turmeric (Figs. 7 and 9) were Stachyurin, 1-o-Caffeoylglucose, trans-o-Coumaric acid 2-glucoside, l-Arabinose, and Isorhamnetin, which had maximum binding energy ranging from −11.87 to −6.965 kcal/mol and Curcuminoid, (-)-Isoborneol, Borneol, Curcuminoid, Spathulenol with docking score ranging from −6.179 to −3.809. Hydrogen bonds are formed between amino acids SER 508, SER 363, ASN 414, ARG 415; LEU 557, VAL 463, SER 363, ARG 415, ASN 414, ASN 382; SER 363, SER 602, LEU 365, VAL 604, ILE 416, VAL 463; ALA 510, ILE 416; SER 363, ILE 416 were found to have interacted with the active site of the protein target of the yellow turmeric plant. While Pi-cation and H-Bond at position GLN 530, TYR 525, SER 602, ARG 415; H-bond at position ILE 416; ILE 416, 355; H-bond at position SER 363, SER 506, ARG 415 and Pi-Pi stacking at position PHE 478; and H-bond at position SER 602 respectively.

4.5. ADMETox property

The term "ADMET" refers to a drug's features of absorption, distribution, metabolism, excretion, and toxicity. Due to their ability to affect a drug's safety, efficacy, and overall therapeutic potential, these characteristics are crucial factors to consider during the development and assessment of novel medications. To evaluate a drug's ADMET qualities, a variety of instruments and methods can be utilized. A few of these are: A compound's polar surface area (PSA), which is the sum of all the polar atoms (atoms having a partial positive or negative charge) on the surface of the compound, is measured [58]. Because polar substances tend to be more soluble in polar solvents and more permeable through biological membranes, PSA is frequently employed as a predictor of the solubility and permeability of a chemical [59].

Overall, PSA should be considered when assessing a compound's characteristics since it affects the compound's solubility, permeability, and overall biological activity. A computational tool called Qplog BB (QSAR Model for Blood-Brain Barrier Permeation) employs machine learning techniques to forecast whether a medicine will cross the blood-brain barrier [60]. A computer approach called PISA (Protein Inhibitor Stability Algorithm) may be used to forecast the likelihood of drug-drug interactions by forecasting the stability of protein-ligand interactions. The "rule of five" suggests that a medication is more likely to be absorbed orally if it satisfies a set of requirements, such as having a molecular weight below 500, a log P (octanol-water partition coefficient) below 5, and having less than 10 hydrogen bond donors and acceptors. Qplog HERG is an algorithmic tool that employs machine learning to foretell if a medicine would block the HERG potassium channel, which can cause cardiac toxicity [61].

A computational method called QPPCaco (Quantitative Prediction of Permeability and Absorption in the Caco-2 Cell Line) employs machine learning algorithms to forecast a drug's permeability and absorption in the Caco-2 cell line, a popular model for intestinal drug absorption. The ADMET qualities of medicine may be predicted, evaluated, and identified using these tools and methods, as well as any possible risks or liabilities that may need to be taken into consideration throughout the drug development process. To predict a compound's permeability and absorption in the Madin-Darby Canine Kidney (MDCK) cell line, a widely used model for intestinal drug absorption, the computational tool QPPMDCK (Quantitative Prediction of Permeability and Absorption in the Madin-Darby Canine Kidney Cell Line) uses machine learning algorithms [62]. The computational tool QplogKp (QSAR Model for Plasma Protein Binding) employs machine learning methods to predict a compound's affinity for plasma proteins, which may affect the compound's distribution and clearance in the body [63].

A hydrogen atom that is covalently attached to a highly electronegative atom (such as oxygen or nitrogen) and may be given up to establish a hydrogen bond with another molecule is known as a donor hydrogen bond (HB). Because they may impact a molecule's stability, shape, and function, hydrogen bonds play a crucial role in biology. Medicine is more likely to be orally accessible if it satisfies the "rule of three" parameters, which include having a molecular weight under 500, a log P (octanol-water partition coefficient) below 3, and less than 10 hydrogen bond donors and acceptors. The rationale for this recommendation is that medications having these characteristics are more likely to pass past the intestinal wall and enter the bloodstream.

4.6. Ramachandran plot

In silico methods, specifically molecular docking, play a crucial role in predicting ligand binding affinities to cardiac proteins. However, to comprehensively understand the structure-function relationship of these proteins, the inclusion of a Ramachandran plot analysis becomes imperative. The conformations of polypeptide chains in proteins are graphically represented by Ramachandran plots, also called Ramachandran diagrams. For examining and predicting the protein structures of amino acid residues, it is a valuable tool. In a Ramachandran plot as shown in Fig. 10, the x-axis represents the phi angle (φ) and the y-axis represents the psi angle (ψ). The phi angle is the angle between the C—N bond and the C—C bond in the peptide backbone, while the psi angle is the angle between the N—Cα bond and the Cα-C bond. The most frequent conformations of the polypeptide chain are shown by the area of the plot with the highest density of dots. Outside of this area, conformations are less frequent and can be regarded as forbidden or abnormal. The most stable protein conformations may be found using Ramachandran plots, as well as any conformations that might be unstable or prone to structural alterations [64]. They are a useful tool for comprehending the structure and function of proteins and are often employed in the field of protein research. Lastly, it provides a visual representation of the backbone dihedral angles (phi and psi) of the amino acid residues of the protein of study, highlighting regions of energetically favorable and unfavorable conformations. The inclusion of Ramachandran plot analysis is crucial for ensuring the reliability of the protein structures utilized in the molecular docking simulations performed in this study.

From the results generated in this study, the *in silico* study showed that CL has high binding affinity for Nrf2 which is an important component in antioxidant defenses and may serve as a potent cardioprotective agent. CZ on the other hand showed improved physicochemical properties and drug-likeness better than what was seen in CL. This finding complements the results generated from the *in vivo* study as the plant was able to demonstrate cardio-protective effects against

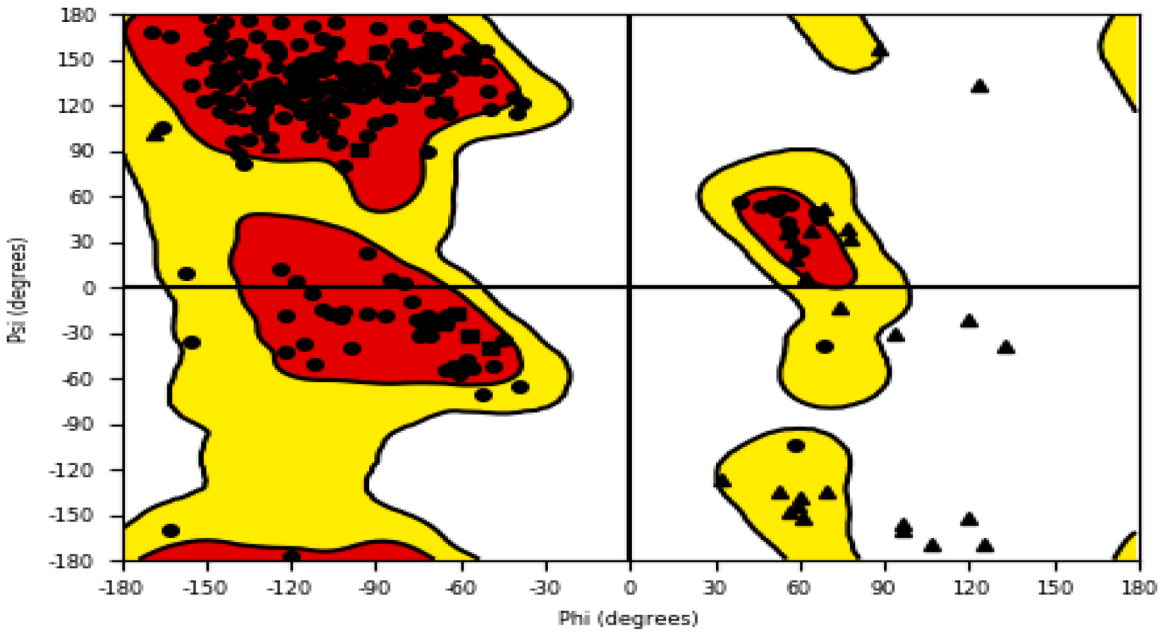

Fig. 10. Shows the Ramachandran plot's Phi= 87.8 and Psi= 157.9°. Residue A: GLY 430.

cardio oxidative stress by modulating the effects of manganese toxicity on the heart [40].

Similarly to what we identified, stachyurin was identified in a traditional Chinese herbal preparation called Liu Wei Di Huang Wan, which is commonly used to treat kidney and liver diseases [65]. The other compounds listed are also found in traditional Chinese herbal preparations, such as: - 1-o-Caffeoyl Glucose is found in Gegen Qinlian Decoction, which is used to treat digestive disorders and - trans-o-Coumaric acid 2-glucoside is found in Sho-Saiko-To [66]. This compound is used to treat liver diseases and inflammation. Also, a variety of literature have identified these compounds in Chinese herbal preparations, including: - l-Arabinose which is found in Danggui Buxue Tang, and used to treat various gynecological conditions [67]. Isorhamnetin is found in Yin Chen Hao Tang, which is used to treat liver disease [68]. Curcuminoid compounds which are one of the most prevalent in both species are found in Jian-Pi-Yi-Qi Tang, a traditional Chinese herbal preparation that is used to treat indigestion, gastritis, and other gastrointestinal disorders [69,70]. Isoborneol and borneol are both found in Xiao Chai Hu Tang, which is used to treat liver disease, inflammation, and fevers [71]. Lastly, spathulenol is found in Yu Ping Feng San, which is used to strengthen the immune system [72]. These reports point to the rich history of Chinese herbal medicine and the in silico identification of these phytochemicals in this study.

5. Limitations and strengths of the study

This study has some limitations that should be acknowledged to ensure a comprehensive understanding of the research findings. The limitations are as follows:

i. Small Sample Size: The study used a small sample size ($n = 5$) for each experimental group. A larger sample size would enhance the statistical power and generalizability of the findings. The small sample size may limit the robustness of the conclusions drawn from the study.
ii. Animal Model Limitations: The study used rats as an animal model to investigate the effects of turmeric rhizome extracts on manganese toxicity. While animal models provide valuable insights, extrapolating these findings to humans requires caution due to potential species differences in metabolism and response to interventions.
iii. Single Dose Levels: The study evaluated the effects of specific doses of turmeric extracts, and it may not capture potential dose-dependent responses. A broader range of doses should be considered to establish dose-response relationships and identify optimal therapeutic concentrations.
iv. Short Duration of Treatment: The duration of treatment in the study might not be sufficient to observe long-term effects or potential adverse outcomes. Chronic exposure to turmeric extracts and monitoring over an extended period could provide a more comprehensive understanding of their effects.
v. Limited Biochemical Parameters: While the study assessed several biochemical parameters related to oxidative stress, it may benefit from exploring additional markers to obtain a more comprehensive understanding of the mechanisms involved in the cardioprotective effects of turmeric extracts.
vi. Limited Clinical Relevance: While the study provides valuable insights into the potential cardioprotective effects of turmeric extracts, the translation of these findings to clinical applications in humans requires additional research and clinical trials.

On the other hand, the strength of this study lies in its multi-faceted approach, combining in-vivo experiments with in-silico analyses and providing a thorough examination of the cardioprotective effects of turmeric rhizome extracts. The strengths of the study are enumerated below:

i. Comprehensive Biochemical Assessment: The study evaluates multiple biochemical parameters related to oxidative stress and antioxidant defense mechanisms. By assessing GSH levels, LPO, antioxidant power, NO levels, and SOD activity, the research provides a comprehensive understanding of the impact of turmeric rhizome extracts on manganese-induced cardiotoxicity.
ii. Dose-Dependent Effects: The study examines the effects of different doses of turmeric extracts on the biochemical parameters. This dose-dependent analysis allows for a nuanced understanding of how varying concentrations of CL and CZ contribute to the observed changes in GSH, LPO, antioxidant power, NO, and SOD activity.

iii. Comparative Analysis: The comparison between CL and CZ adds depth to the research, enabling insights into potential variations in the cardioprotective effects of different turmeric species. This comparative analysis contributes to the broader understanding of turmeric's therapeutic potential.
iv. In-silico Studies: The incorporation of in-silico studies, including molecular docking and MM/GBSA analysis, enhances the research by providing a molecular and structural-level perspective on the interactions between turmeric compounds and the Nrf2 protein. This computational approach supports and complements the *in vivo* findings.
v. Future Implications: The study opens avenues for future research by suggesting that further investigation and structural modifications of specific turmeric compounds, such as stachyurin, could lead to the development of potent drugs for mitigating manganese-induced cardiotoxicity.
vi. ADMET Analysis: The inclusion of ADMET analysis using computational tools adds value by assessing the pharmacokinetic and toxicity properties of the turmeric compounds. This information is crucial for understanding the potential translational applications of these compounds.

6. Conclusion

In conclusion, this study demonstrated that the selected turmeric (*Curcuma longa and Curcuma zedoaria*) exhibits cardio-protective effects against cardio oxidative stress by modulating the effects of manganese toxicity on the heart, and the mechanism of action by which they exert this effect could be due to their antioxidant and anti-inflammatory properties. To identify promising new phytochemicals to activate nuclear factor erythroid 2-related factor 2 (Nrf2), a target protein involved in controlling antioxidant enzymes, bioactive compounds of *Curcuma longa* and *Curcuma zedoaria* were screened in this study using a combination of ADMET and structure-based virtual screening followed by binding energy estimation. The lead compounds in CL showed higher free binding energy and a higher binding affinity for the protein compared to CZ and competed well against the co-crystallize ligand. The outcome of the molecular docking revealed that lead compounds produced H-bond interactions with ARG 415 and SER 602 that were identical to those of the co-crystallized ligand. The lead compounds' drug-likeness was also predicted, and CZ was shown to be less toxic compared to CL as they broke Lipinski's rule of five and Jorgensen's rule of three. The suggested group of ligands demonstrated effective Nrf2 agonistic activity in the *in-silico* study, and therefore, they can be used in future research to expand the findings to experimental verification.

Funding

This research did not receive any specific grant from funding agencies in the public, commercial, or not-for-profit sectors.

CRediT authorship contribution statement

Toluwalope T. Fasooto: Writing – review & editing, Writing – original draft, Resources, Project administration, Methodology, Investigation, Formal analysis, Conceptualization. **Oluwakemi R. Ogundana:** Writing – review & editing, Validation, Resources, Methodology, Investigation. **Abiola F. Adebayo:** Writing – original draft, Methodology, Investigation, Data curation. **David B. Olawade:** Writing – review & editing, Writing – original draft, Resources, Formal analysis. **Ezekiel A. Olugbogi:** Writing – review & editing, Writing – original draft, Software, Formal analysis. **Oluwaseun Fapohunda:** Writing – review & editing, Writing – original draft, Resources. **Afolabi C. Akinmoladun:** Writing – review & editing, Supervision, Methodology, Investigation.

Declaration of competing interest

The authors declare that they have no known competing financial interests or personal relationships that could have appeared to influence the work reported in this paper.

Data availability

Data will be made available on request.

References

[1] R. Lucchini, D. Placidi, G. Cagna, C. Fedrighi, M. Oppini, M. Peli, S. Zoni, Manganese and developmental neurotoxicity. Neurotoxicity of Metals, 2017, pp. 13–34.
[2] L. Li, X. Yang, The essential element manganese, oxidative stress, and metabolic diseases: links and interactions, Oxid. Med. Cell Longev. 2018 (2018).
[3] E. Walter, S. Alsaffar, C. Livingstone, S.L. Ashley, Manganese toxicity in critical care: case report, literature review, and practice recommendations, J. Intensive Care Soc. 17 (3) (2016) 252–257.
[4] S.L. O'Neal, W. Zheng, Manganese toxicity upon overexposure: a decade in review, Curr. Environ. Health Rep. 2 (2015) 315–328.
[5] S. Dikalov, H. Itani, B. Richmond, L. Arslanbaeva, A. Vergeade, S.J. Rahman, O. Boutaud, T. Blackwell, P.P. Massion, D.G. Harrison, A. Dikalova, Tobacco smoking induces cardiovascular mitochondrial oxidative stress, promotes endothelial dysfunction, and enhances hypertension, Am. J. Physiol. Heart Circ. Physiol. 316 (3) (2019) H639–H646.
[6] E. D'Adamo, O. Guardamagna, F. Chiarelli, A. Bartuli, D. Liccardo, F. Ferrari, V. Nobili, Atherogenic dyslipidemia and cardiovascular risk factors in obese children, Int. J. Endocrinol. 2015 (2015).
[7] T. Farkhondeh, S. Samarghandian, Antidotal effects of curcumin against agents-induced cardiovascular toxicity, Cardiovas. Haematol. Disorders-Drug Targets 16 (1) (2016) 30–37 (Formerly Current Drug Targets-Cardiovascular & Hematological Disorders).
[8] T.J. Anderson, J. Grégoire, G.J. Pearson, A.R. Barry, P. Couture, M. Dawes, G. A. Francis, J. Genest Jr., S. Grover, M. Gupta, R.A. Hegele, 2016 Canadian Cardiovascular Society guidelines for the management of dyslipidemia for the prevention of cardiovascular disease in adults, Can. J. Cardiol. 32 (11) (2016) 1263–1282.
[9] W. Zhang, N. Cui, J. Ye, B. Yang, Y. Sun, H. Kuang, Curcumin's prevention of inflammation-driven early gastric cancer and its molecular mechanism, Chin. Herb. Med. 14 (2) (2022) 244–253.
[10] D. Bagenna, H. Wang, Y. Wu, L. Anggelima, Famous traditional Mongolian medicine Xieriga-4 (Turmeric-4) decoction: a review, Chin. Herb. Med. 14 (3) (2022) 385–391.
[11] M. Akaberi, A. Sahebkar, S.A. Emami, Turmeric and curcumin: from traditional to modern medicine. Studies On Biomarkers and New Targets in Aging Research in Iran: Focus on Turmeric and Curcumin, 2021, pp. 15–39.
[12] Y. Li, J. Feng, Y. Mo, H. Liu, B. Yang, Concordance between cardio-protective effect on isoproterenol-induced acute myocardial ischemia and phenolic content of different extracts of Curcuma aromatica, Pharm. Biol. 54 (12) (2016) 3226–3231.
[13] W.E. Nabofa, O.O. Alashe, O.T. Oyeyemi, A.F. Attah, A.A. Oyagbemi, T. O. Omobowale, A.A. Adedapo, A.R. Alada, Cardioprotective effects of curcumin-nisin based poly lactic acid nanoparticle on myocardial infarction in guinea pigs, Sci. Rep. 8 (1) (2018) 16649.
[14] G.M. Morris, M. Lim-Wilby, Molecular docking. Molecular Modeling of Proteins, 2008, pp. 365–382.
[15] P. Setiarso, N. Kusumawati, R. Rusijono, S. Muslim, Optimization of Slice Thickness, Drying Method, and Temperature of Turmeric Rhizome (Curcuma Longa L.) Based on Water Content and Functional Compound Degradation, in: Proceedings of the International Conference on Science and Technology, Atlantis Press, 2018, pp. 46–52, https://doi.org/10.2991/icst-18.2018.10.
[16] E. Beutler, O. Duron, B.M. Kelly, Improved method for the determination of blood glutathione, J. Lab. Clin. Med. 61 (1985) 882–888.
[17] S.B. Patil, N.S. Naikwade, C.S. Magdum, Review on Phytochemistry and Pharmacological Aspects of Euphorbia hirta Linn, J. Pharm. Res. Health Care 1 (1) (2009).
[18] I. Guevara, J. Iwanejko, A. Dembińska-Kieć, J. Pankiewicz, A. Wanat, P. Anna, I. Gołąbek, S. Bartuś, M. Malczewska-Malec, A. Szczudlik, Determination of nitrite/nitrate in human biological material by the simple Griess reaction, Clinicachimica Acta 274 (2) (1998) 177–188.
[19] P. Kakkar, B. Das, P.N. Viswanathan, A modified spectrophotometric assay of superoxide dismutase, Indian J. Biochem. Biophys. 21 (2) (1984).
[20] A.F. Winkel, C.K. Engel, D. Margerie, A. Kannt, H. Szillat, H. Glombik, D. Schmoll, Characterization of RA839, a noncovalent small molecule binder to Keap1 and selective activator of Nrf2 signaling, J. Biol.Chem. 290 (47) (2015) 28446–28455.
[21] E.A. Olugbogi, D.S. Bodun, S.D. Omoseeye, A.O. Onoriode, F.O. Oluwamoroti, J. F. Adedara, I.A. Oriyomi, F.O. Bello, F.O. Olowoyeye, O.G. Laoye, D.B. Adebowale, Quassia amara bioactive compounds as a Novel DPP-IV inhibitor: an in-silico study, Bull. Natl. Res. Cent. 46 (1) (2022) 1–14.

[22] J. Zhang, X. Ma, W. Wang, X. Wu, B. Ma, C. Yu, H. Wang, Three new sesquiterpenes from roots of Curcuma longa, Chin. Herb. Med. 15 (3) (2023) 470–474.
[23] N. Abdel-Magied, N. Abdel-Aziz, S.M. Shedid, A.G. Ahmed, Modulating effect of tiron on the capability of mitochondrial oxidative phosphorylation in the brain of rats exposed to radiation or manganese toxicity, Environ. Sci. Pollut. Res. 26 (2019) 12550–12562.
[24] N. Aziz, A. Sharif, A. Raza, K. Jermsittiparsert, The role of natural resources, globalization, and renewable energy in testing the EKC hypothesis in MINT countries: new evidence from Method of Moments Quantile Regression approach, Environ. Sci. Pollut. Res. 28 (2021) 13454–13468.
[25] Y.M. Jiang, X.A. Mo, F.Q. Du, X. Fu, X.Y. Zhu, H.Y. Gao, J.L. Xie, F.L. Liao, E. Pira, W. Zheng, Effective treatment of manganese-induced occupational Parkinsonism with p-aminosalicylic acid: a case of 17-year follow-up study, J. Occup. Environ. Med./Am. College Occup. Environ. Med. 48 (6) (2006) 644.
[26] X.F. Liu, L.M. Zhang, H.N. Guan, Z.W. Zhang, S.W. Xu, Effects of oxidative stress on apoptosis in manganese-induced testicular toxicity in cocks, Food Chem. Toxicol. 60 (2013) 168–176.
[27] L. Zeng, T. Yang, K. Yang, G. Yu, J. Li, W. Xiang, H. Chen, Efficacy and safety of curcumin and curcuma longa extract in the treatment of arthritis: a systematic review and meta-analysis of randomized controlled trial, Front. Immunol. 13 (2022) 891822.
[28] Y. Jia, X. Li, Q. Liu, X. Hu, J. Li, R. Dong, P. Liu, G. Liu, L. Luo, Z. Chen, Physiological and transcriptomic analyses reveal the roles of secondary metabolism in the adaptive responses of Stylosanthes to manganese toxicity, BMC. Genomics 21 (2020) 1–17.
[29] W. Zheng, Q. Zhao, V. Slavkovich, M. Aschner, J.H. Graziano, Alteration of iron homeostasis following chronic exposure to manganese in rats, Brain Res. 833 (1) (1999) 125–132.
[30] M. Alizadeh, S. Kheirouri, Curcumin reduces malondialdehyde and improves antioxidants in humans with diseased conditions: a comprehensive meta-analysis of randomized controlled trials, Biomedicine 9 (4) (2019).
[31] D.D. Mruk, B. Silvestrini, M.Y. Mo, C.Y. Cheng, Antioxidant superoxide dismutase-a review: its function, regulation in the testis, and role in male fertility, Contraception 65 (4) (2002) 305–311.
[32] S.S. Ali, J.I. Hardt, L.L. Dugan, SOD activity of carboxyfullerenes predicts their neuroprotective efficacy: a structure-activity study, Nanomed.: Nanotechnol. Biol. Med. 4 (4) (2008) 283–294.
[33] A.L. Levonen, M. Inkala, T. Heikura, S. Jauhiainen, H.K. Jyrkkänen, E. Kansanen, K. Määttä, E. Romppanen, P. Turunen, J. Rutanen, S. Ylä-Herttuala, Nrf2 gene transfer induces antioxidant enzymes suppresses smooth muscle cell growth *in vitro* and reduces oxidative stress in rabbit aorta *in vivo*, Arterioscler. Thromb. Vasc. Biol. 27 (4) (2007) 741–747.
[34] X. Wang, The expanding role of mitochondria in apoptosis, Genes Dev. 15 (22) (2001) 2922–2933.
[35] J. Lee, J. Jang, S.M. Park, S.R. Yang, An update on the role of Nrf2 in respiratory disease: molecular mechanisms and therapeutic approaches, Int. J. Mol. Sci. 22 (16) (2021) 8406.
[36] Y. Chen, M.B. Azad, S.B. Gibson, Superoxide is the major reactive oxygen species regulating autophagy, Cell Death Differentiation 16 (7) (2009) 1040–1052.
[37] S. Tekin, E. Seven, Assessment of serum catalase reduced glutathione, and superoxide dismutase activities and malondialdehyde levels in keratoconus patients, Eye 36 (10) (2022) 2062–2066.
[38] J.A. Ezugwu, U.C. Okoro, M.A. Ezeokonkwo, K.S. Hariprasad, M. Rudrapal, D. I. Ugwu, O.C. Ekoh, Design, synthesis, molecular docking, molecular dynamics, and *in vivo* antimalarial activity of new dipeptide-sulfonamides, ChemistrySelect. 7 (5) (2022) e202103908.
[39] I.M. Othman, M.H. Mahross, M.A. Gad-Elkareem, M. Rudrapal, N. Gogoi, D. Chetia, A. Kadri, Toward a treatment of antibacterial and antifungal infections: design, synthesis and *in vitro* activity of novel arylhydrazothiazolylsulfonamides analogs and their insight of DFT, docking and molecular dynamic simulations, J. Mol. Struct. 1243 (2021) 130862.
[40] R. Baru Venkata, D.S.N.B.K. Prasanth, P.K. Pasala, S.P. Panda, V.B. Tatipamula, S. Mulukuri, J.K. Kammili, Utilizing Andrographis paniculata leaves and roots by effective usage of the bioactive andrographolide and its nanodelivery: investigation of antikindling and antioxidant activities through in silico and *in vivo* studies, Front. Nutr. 10 (2023) 1185236.
[41] A.R. Issahaku, E.Y. Salifu, C. Agoni, M.I. Alahmdi, N.E. Abo-Dya, M.E. Soliman, N. Podila, Discovery of potential KRAS-SOS1 Inhibitors from south african natural compounds: an in silico approach, ChemistrySelect 8 (24) (2023) e202300277.
[42] K.M. Kim, S.H. Ki, Nrf2: a key regulator of redox signaling in liver diseases. Liver Pathophysiology, Academic Press, 2017, pp. 355–374.
[43] M. Rudrapal, W.A. Eltayeb, G. Rakshit, et al., Dual synergistic inhibition of COX and LOX by potential chemicals from Indian daily spices investigated through detailed computational studies, Sci. Rep. 13 (2023) 8656, https://doi.org/10.1038/s41598-023-35161-0.
[44] E. Olugbogi, O. Arobadade, S. Balogun, H. Akingbola, O. Adelakun, T. Popoola, L. Arietarhire, Application of in-silico methodologies in exploring the antagonistic potential of trigonella foenum-graecum on cyclooxygenase-2 (Cox-2) in cancer treatment, IPS J. Mol. Dock. Simul. 2 (1) (2023) 26–36.
[45] D. James, M.D. Cherry, Normal and Impaired Immunologic Responses to Infection. Glutathione Peroxidase. Feigin and Cherry's Textbook of Pediatric Infectious Diseases, 2019, 2019.
[46] Y. Cao, G. Jiang, M. Li, X. Fang, D. Zhu, W. Qiu, J. Zhu, D. Yu, Y. Xu, Z. Zhong, J. Zhu, Glutaredoxins play an important role in the redox homeostasis and symbiotic capacity of azorhizobiumcaulinodans ORS571, Mol. Plant-Microbe Inter. 33 (12) (2020) 1381–1393.
[47] F. He, X. Ru, T. Wen, NRF2, a transcription factor for stress response and beyond, Int. J. Mol. Sci. 21 (13) (2020) 4777.
[48] B.D. Cameron, K.R. Sekhar, M. Ofori, M.L. Freeman, The role of Nrf2 in the response to normal tissue radiation injury, Radiat. Res. 190 (2) (2018) 99–106.
[49] V. Guleria, T. Pal, B. Sharma, S. Chauhan, V. Jaiswal, Pharmacokinetic and molecular docking studies to design antimalarial compounds targeting Actin I, Int. J. Health Sci. 15 (6) (2021) 4.
[50] E.A. Olugbogi, O.I. Omotuyi, K.T. Mesileya, D.S. Bodun, S.D. Omoseeye, A. O. Onoriode, P.C. Onyeka, Computer based screening of the anticancer property of selected panax ginseng phyto-ligands, Int. J. Pharm. Sci. Res. 14 (4) (2023) 1714–1727.
[51] C. Huerta, X. Jiang, I. Trevino, C.F. Bender, D.A. Ferguson, B. Probst, W.C. Wigley, Characterization of novel small-molecule NRF2 activators: structural and biochemical validation of stereospecific KEAP1 binding, Biochim. Biophys. Acta (BBA)-General Subjects 1860 (11) (2016) 2537–2552.
[52] P. Mignon, S. Loverix, J. Steyaert, P. Geerlings, Influence of the π–π interaction on the hydrogen bonding capacity of stacked DNA/RNA bases, Nucleic Acids Res. 33 (6) (2005) 1779–1789.
[53] S. Genheden, O. Kuhn, P. Mikulskis, D. Hoffmann, U. Ryde, The normal-mode entropy in the MM/GBSA method: effect of system truncation, buffer region, and dielectric constant, J. Chem. Inf. Model. 52 (8) (2012) 2079–2088.
[54] A.R. Issahaku, N. Mukelabai, C. Agoni, et al., Characterization of the binding of MRTX1133 as an avenue for the discovery of potential KRASG12D inhibitors for cancer therapy, Sci. Rep. 12 (2022) 17796, https://doi.org/10.1038/s41598-022-22668-1.
[55] F. Stanzione, I. Giangreco, J.C. Cole, Use of molecular docking computational tools in drug discovery, Prog. Med. Chem. 60 (2021) 273–343.
[56] J. Bostrom, C.V. Lee, L. Haber, G. Fuh, Therapeutic antibodies, methods and protocols, Methods Mol. Biol. 525 (2008) 353–376.
[57] J. Li, R. Abel, K. Zhu, Y. Cao, S. Zhao, R.A. Friesner, The VSGB 2.0 model: a next-generation energy model for high-resolution protein structure modeling, Proteins: Struct. Funct. Bioinformatics 79 (10) (2011) 2794–2812.
[58] L.L. Ferreira, A.D. Andricopulo, ADMET modeling approaches in drug discovery, Drug Discov. Today 24 (5) (2019) 1157–1165.
[59] H. Pajouhesh, G.R. Lenz, Medicinal chemical properties of successful central nervous system drugs, NeuroRx. 2 (2005) 541–553.
[60] A.A. Toropov, A.P. Toropova, M. Beeg, M. Gobbi, M. Salmona, QSAR model for blood-brain barrier permeation, J. Pharmacol. Toxicol. Methods 88 (2017) 7–18.
[61] K.M. Thai, G.F. Ecker, A binary QSAR model for classification of hERG potassium channel blockers, Bioorg. Med. Chem. 16 (7) (2008) 4107–4119.
[62] J.D. Irvine, L. Takahashi, K. Lockhart, J. Cheong, J.W. Tolan, H.E. Selick, J. R. Grove, MDCK (Madin–Darby canine kidney) cells: a tool for membrane permeability screening, J. Pharm. Sci. 88 (1) (1999) 28–33.
[63] T. Ghafourian, Z. Amin, QSAR models for the prediction of plasma protein binding, BioImpacts: BI 3 (1) (2013) 21.
[64] V. Morea, A. Tramontano, M. Rustici, C. Chothia, A.M. Lesk, Conformations of the third hypervariable region in the VH domain of immunoglobulins, J. Mol. Biol. 275 (2) (1998) 269–294.
[65] Y. Wang, Y. Zhao, X. Liu, J. Li, J. Zhang, D. Liu, Chemical constituents and pharmacological activities of medicinal plants from Rosa genus, Chin. Herb. Med. 14 (2) (2022) 187–209.
[66] X. Nöst, E.M. Pferschy-Wenzig, X.T. Yu, M. Li, X.L. Tong, R. Bauer, Comprehensive metabolic profiling of modified gegen qinlian decoction by ultra-high-performance liquid chromatography-diode array detection-Q-exactive-orbitrap-electrospray ionization-mass spectrometry/mass spectrometry and application of high-performance thin-layer chromatography for its fingerprint analysis, World J. Tradit. Chin. Med. 7 (1) (2021) 11–32.
[67] Y. Chen, J.A. Duan, D. Qian, J. Guo, B. Song, M. Yang, Assessment and comparison of immunoregulatory activity of four hydrosoluble fractions of Angelica sinensis *in vitro* on the peritoneal macrophages in ICR mice, Int. Immunopharmacol. 10 (4) (2010) 422–430.
[68] G. Gong, Y.Y. Guan, Z.L. Zhang, K. Rahman, S.J. Wang, S. Zhou, H. Zhang, Isorhamnetin: a review of pharmacological effects, Biomed. Pharmacother. 128 (2020) 110301.
[69] K.H. Lee, S.L. Morris-Natschke, X. Yang, R. Huang, T. Zhou, S.F. Wu, H. Itokawa, Recent progress of research on medicinal mushrooms, foods, and other herbal products used in traditional Chinese medicine, J. Tradit. Complement. Med. 2 (2) (2012) 1–12.
[70] S. Sen, R. Chakraborty, Herbs, gastrointestinal protection, and oxidative stress. Gastrointestinal Tissue, Academic Press, 2017, pp. 259–274.
[71] Y. Li, M. Ren, J. Wang, R. Ma, H. Chen, Q. Xie, J. Wang, Progress in borneol intervention for ischemic stroke: a systematic review, Front. Pharmacol. 12 (2021) 606682.
[72] Y. Bai, W. Wei, C. Yao, S. Wu, W. Wang, D.A. Guo, Advances in the chemical constituents, pharmacological properties and clinical applications of TCM formula Yupingfeng San, Fitoterapia 164 (2023) 105385.